J|A|C|S
ARTICLES
Published on Web 01/24/2007

Chiral Phosphine−Olefin Ligands in the Rhodium-Catalyzed Asymmetric 1,4-Addition Reactions

Wei-Liang Duan,[†] Hiroshi Iwamura,[‡] Ryo Shintani,*[,†] and Tamio Hayashi*[,†]

Contribution from the Department of Chemistry, Graduate School of Science, Kyoto University, Sakyo, Kyoto 606-8502, Japan, and Mitsubishi Pharma Corporation, Kamisu, Ibaraki 314-0255, Japan

Received October 4, 2006; E-mail: shintani@kuchem.kyoto-u.ac.jp; thayashi@kuchem.kyoto-u.ac.jp

Abstract: A full overview on the use of chiral phosphine−olefin ligands **1** in the rhodium-catalyzed asymmetric 1,4-addition of arylboronic acids to α,β-unsaturated carbonyl compounds is described. Effective chiral environment of a Rh/**1** complex was shown to resemble that of a Rh/(*R*,*R*)-Ph-bod* complex by comparing the experimental results as well as the X-ray crystal structures. High catalytic activity of a Rh/**1** complex was disclosed and the catalytic cycle involving a trimer−monomer equilibrium was established through mechanistic studies using a reaction calorimeter and ^{31}P NMR spectroscopy. A negative nonlinear effect derived from an inactive trimer−active monomer equilibrium of the catalyst was also successfully observed.

Introduction

Asymmetric transformations catalyzed by transition-metal complexes coordinated with chiral ligands are powerful methods for constructing chiral enantio-enriched compounds using achiral substrates and reagents. The design and the synthesis of new chiral ligands are, therefore, very important in advancing asymmetric catalysis. Conventional chiral ligands for late transition-metals are typically based on phosphorus- and/or nitrogen-coordination, and several ligands have proved to be highly effective for various asymmetric reactions.[1] For example, binap,[2] an axially chiral bisphosphine ligand, has found a wide range of applications in combination with several transition metals,[3] and the chiral environment of a metal/binap complex is usually controlled by the face/edge orientations of the phenyl groups on the phosphorus atoms as illustrated in Figure 1a.

As conceptually new chiral ligands, a series of chiral dienes have been developed in the past few years, proving that good chiral environments can be created around olefin ligands.[4,5,6] In particular, our group has focused on the development of C_2-symmetric bicyclic dienes such as (*R*,*R*)-Ph-bod*,[5] whose chiral environment is derived from the steric difference between the phenyl group and the hydrogen atom on the olefins (Figure 1b). This mode of space discrimination around the central metal is drastically different from that of binap in that the chirality is rigidly controlled by the size of the substituents rather than by the conformational differentiation. This rigid feature also makes it easy to predict the stereochemical outcome of the reactions taking place on the metal/chiral diene complex. Furthermore, we have found that chiral diene ligands provide highly active catalysts in the rhodium-catalyzed 1,4-addition reactions.[4g]

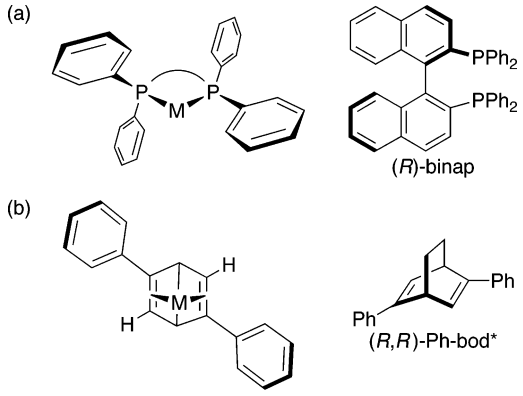

Figure 1. Comparison of the chiral environment between (a) metal/(*R*)-binap complex and (b) metal/(*R*,*R*)-Ph-bod* complex.

[†] Kyoto University.
[‡] Mitsubishi Pharma Corporation.

(1) (a) Ojima, I., Ed. *Catalytic Asymmetric Synthesis*, 2nd ed; Wiley-VCH: New York, 2000. (b) Jacobsen, E. N., Pfaltz, A., Yamamoto, H., Eds. *Comprehensive Asymmetric Catalysis I-III*; Springer-Verlag: New York, 1999.
(2) Takaya, H.; Mashima, K.; Koyano, K.; Yagi, M.; Kumobayashi, H.; Taketomi, T.; Akutagawa, S.; Noyori, R. *J. Org. Chem.* **1986**, *51*, 629.
(3) For reviews, see: (a) Noyori, R.; Takaya, H. *Acc. Chem. Res.* **1990**, *23*, 345. (b) Akutagawa, S. *Appl. Catal. A: Gen.* **1995**, *128*, 171. (c) McCarthy, M.; Guiry, P. J. *Tetrahedron* **2001**, *57*, 3809. (d) Shimizu, H.; Nagasaki, I.; Saito, T. *Tetrahedron* **2005**, *61*, 5405.
(4) (a) Hayashi, T.; Ueyama, K.; Tokunaga, N.; Yoshida, K. *J. Am. Chem. Soc.* **2003**, *125*, 11508. (b) Shintani, R.; Ueyama, K.; Yamada, I.; Hayashi, T. *Org. Lett.* **2004**, *6*, 3425. (c) Otomaru, Y.; Tokunaga, N.; Shintani, R.; Hayashi, T. *Org. Lett.* **2005**, *7*, 307. (d) Shintani, R.; Okamoto, K.; Otomaru, Y.; Ueyama, K.; Hayashi, T. *J. Am. Chem. Soc.* **2005**, *127*, 54. (e) Shintani, R.; Tsurusaki, A.; Okamoto, K.; Hayashi, T. *Angew. Chem., Int. Ed.* **2005**, *44*, 3909. (f) Hayashi, T.; Tokunaga, N.; Okamoto, K.; Shintani, R. *Chem. Lett.* **2005**, 1480. (g) Chen, F.-X.; Kina, A.; Hayashi, T. *Org. Lett.* **2006**, *8*, 341. (h) Otomaru, Y.; Kina, A.; Shintani, R.; Hayashi, T. *Tetrahedron: Asymmetry* **2005**, *16*, 1673. (i) Kina, A.; Ueyama, K.; Hayashi, T. *Org. Lett.* **2005**, *7*, 5889.
(5) (a) Tokunaga, N.; Otomaru, Y.; Okamoto, K.; Ueyama, K.; Shintani, R.; Hayashi, T. *J. Am. Chem. Soc.* **2004**, *126*, 13584. (b) Otomaru, Y.; Okamoto, K.; Shintani, R.; Hayashi, T. *J. Org. Chem.* **2005**, *70*, 2503. (c) Shintani, R.; Kimura, T.; Hayashi, T. *Chem. Commun.* **2005**, 3213. (d) Shintani, R.; Okamoto, K.; Hayashi, T. *Chem. Lett.* **2005**, 1294. (e) Shintani, R.; Okamoto, K.; Hayashi, T. *Org. Lett.* **2005**, *7*, 4757. (f) Nishimura, T.; Yasuhara, Y.; Hayashi, T. *Org. Lett.* **2006**, *8*, 979. (g) Shintani, R.; Duan, W.-L.; Hayashi, T. *J. Am. Chem. Soc.* **2006**, *128*, 5628.

10.1021/ja0671013 CCC: $37.00 **© 2007 American Chemical Society**

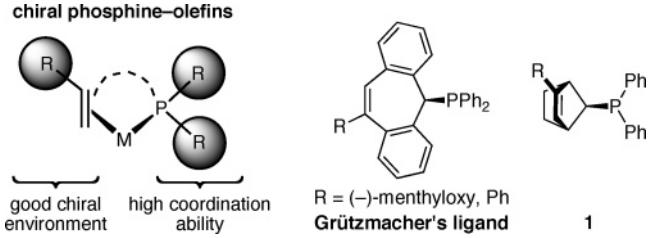

Figure 2. Design of chiral phosphine−olefin ligands (left) and the literature examples (right).

Scheme 1[a]

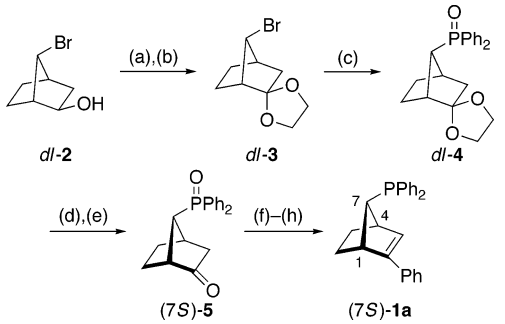

[a] Conditions: (a) oxalyl chloride, DMSO, Et_3N, CH_2Cl_2, 96%. (b) cat. TsOH, ethylene glycol, C_6H_6, 94%. (c) (i) *t*-BuLi, THF; then $ClPPh_2$; (ii) H_2O_2*aq*, acetone, 63% (over two steps). (d) chiral HPLC resolution (OD-H column). (e) 1 N HCl*aq*, THF, 99%. (f) LDA, THF; then $PyNTf_2$, 89%. (g) cat. $PdCl_2$(dppf), PhMgBr, Et_2O, 86%. (h) $HSiCl_3$, Et_3N, C_6H_6, 84%.

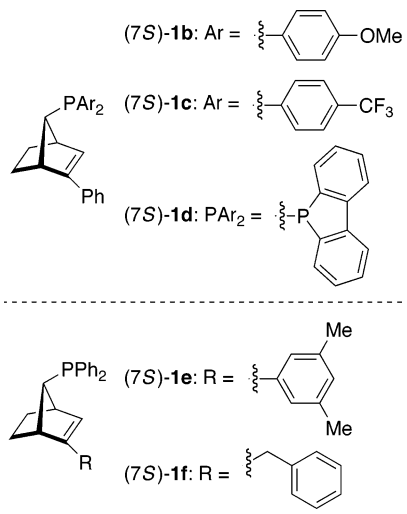

Unfortunately, however, diene ligands generally coordinates to transition-metals more weakly compared to phosphorus-based ligands. To further enhance the utility of chiral olefin ligands with increased coordination ability to transition-metals, we envisioned that the development of a phosphine−olefin hybrid ligand with chirality on the olefin would be an attractive target (Figure 2). In 2004, during the course of our study toward this goal, Grützmacher introduced the first chiral phosphine−olefins on the basis of a dibenzocycloheptatriene framework and utilized them in the iridium-catalyzed asymmetric hydrogenation reactions.[7] We subsequently reported the development of structurally compact phosphine−olefins **1**, which have a bicyclo[2.2.1]-heptene backbone with high rigidity, and demonstrated that they are highly effective ligands for the rhodium-catalyzed asymmetric 1,4-addition of arylboronic acids to maleimides.[8] Here we describe a full overview of the rhodium-catalyzed asymmetric 1,4-addition reactions by the use of this class of phosphine−olefin ligands, including the detailed mechanistic studies.

$$\frac{3}{2}\,[\mathrm{Rh(OH)(cod)}]_2 + 3\ (7S)\text{-}\mathbf{1a} \xrightarrow[50\ ^\circ\mathrm{C},\ 5\ \mathrm{h}]{C_6H_6} [\mathrm{Rh_3}(\mu\text{-O})(\mu\text{-OH})((7S)\text{-}\mathbf{1a})_3] + \mathrm{H_2O}$$

6: 70% yield (1)

Results and Discussion

Preparation of Chiral Phosphine−Olefins 1. The synthesis of (1*S*,4*R*,7*S*)-7-diphenylphosphino-2-phenylbicyclo[2.2.1]hept-2-ene, phosphine−olefin (7*S*)-**1a**, is described in Scheme 1, starting from racemic (*exo*,*syn*)-7-bromobicyclo[2.2.1]heptan-2-ol[9] (*dl*-**2**). Swern oxidation of *dl*-**2**, followed by ketalization with ethylene glycol, gave *dl*-**3**, which was further converted to phosphine oxide *dl*-**4** by lithiation, phosphination, and oxidation. The enantiomers of *dl*-**4** were resolved by chiral HPLC on a Chiralcel OD-H column, and the ketal protection of (7*S*)-**4** was removed to give enantio-pure ketone (7*S*)-**5**. Conversion of (7*S*)-**5** to its enol triflate, followed by Grignard cross-coupling and reduction with trichlorosilane, completed the synthesis of (7*S*)-(−)-**1a** (36% overall yield). Other phosphine−olefins (7*S*)-**1b**−**f** were also synthesized in a similar manner from the common intermediate *dl*-**3**.

Structure of a Rhodium Complex Coordinated with Phosphine−Olefin 1a. As shown in eq 1, a ligand exchange reaction of $[Rh(OH)(cod)]_2$ with (7*S*)-**1a** in benzene cleanly produced a Rh/**1a** complex (**6**), which was characterized to be a trimeric species $[Rh_3(\mu\text{-O})(\mu\text{-OH})((7S)\text{-}\mathbf{1a})_3]$ by X-ray crystallographic analysis (Figure 3).[10,11] The structure of complex **6** displays a C_3 symmetry with each **1a** acting as a phosphine−olefin bidentate ligand to rhodium (P−Rh−olefin bite angles ∼83°). The axis of C_3 symmetry is at the middle of the Rh(1)−Rh(2)−Rh(3) triangle, passing through two oxygen atoms (O(1) and O(2)), and all of the three diphenylphosphino groups are on the same side of the Rh(1)−Rh(2)−Rh(3) triangular plane (Rh−P = 2.15−2.16 Å). The bond lengths of Rh−O(2) that are trans to phosphorus are significantly longer (2.14−2.15 Å) than the Rh−O(1) distances that are trans to olefin (2.03−2.05 Å), and the O(1)−Rh−O(2) angles are 73−

(6) (a) Fischer, C.; Defieber, C.; Suzuki, T.; Carreira, E. M. *J. Am. Chem. Soc.* **2004**, *126*, 1628. (b) Defieber, C.; Paquin, J.-F.; Serna, S.; Carreira, E. M. *Org. Lett.* **2004**, *6*, 3873. (c) Paquin, J.-F.; Defieber, C.; Stephenson, C. R. J.; Carreira, E. M. *J. Am. Chem. Soc.* **2005**, *127*, 10850. (d) Paquin, J.-F.; Stephenson, C. R. J.; Defieber, C.; Carreira, E. M. *Org. Lett.* **2005**, *7*, 3821. (e) Läng, F.; Breher, F.; Stein, D.; Grützmacher, H. *Organometallics* **2005**, *24*, 2997. (f) Grundl, M. A.; Kennedy-Smith, J. J.; Trauner, D. *Organometallics* **2005**, *24*, 2831.
(7) (a) Maire, P.; Deblon, S.; Breher, F.; Geier, J.; Böhler, C.; Rüegger, H.; Schönberg, H.; Grützmacher, H. *Chem.−Eur. J.* **2004**, *10*, 4198. See also: (b) Piras, E.; Läng, F.; Rüegger, H.; Stein, D.; Wörle, M.; Grützmacher, H. *Chem.−Eur. J.* **2006**, *12*, 5849.
(8) (a) Shintani, R.; Duan, W.-L.; Nagano, T.; Okada, A.; Hayashi, T. *Angew. Chem., Int. Ed.* **2005**, *44*, 4611. See also: (b) Shintani, R.; Duan, W.-L.; Okamoto, K.; Hayashi, T. *Tetrahedron: Asymmetry* **2005**, *16*, 3400.
(9) Zalkow, L. H.; Oehlschlager, A. C. *J. Org. Chem.* **1964**, *29*, 1625.
(10) CCDC-619818 contains the supplementary crystallographic data for this paper. These data can be obtained free of charge from the Cambridge Crystallographic Data Centre via www.ccdc.cam.ac.uk/data_request/cif.
(11) There are several structural reports on this type of trimeric rhodium complexes having a Rh_3O_2 core: (a) Churchill, M. R.; Barkan, M. D.; Atwood, J. D.; Ziller, J. W. *Acta Cryst. Sect. C: Cryst. Struct. Commun.* **1990**, *C46*, 2462. (b) Kuhn, N.; Grathwohl, M.; Nachtigal, C.; Steimann, M.; Henkel, G. *Zeit. Anorg. Allg. Chem.* **2001**, *627*, 2039. (c) Marshall, W. J.; Grushin, V. V. *Organometallics* **2004**, *23*, 3343. (d) Vicente, J.; Gil-Rubio, J.; Bautista, D.; Sironi, A.; Masciocchi, N. *Inorg. Chem.* **2004**, *43*, 5665.

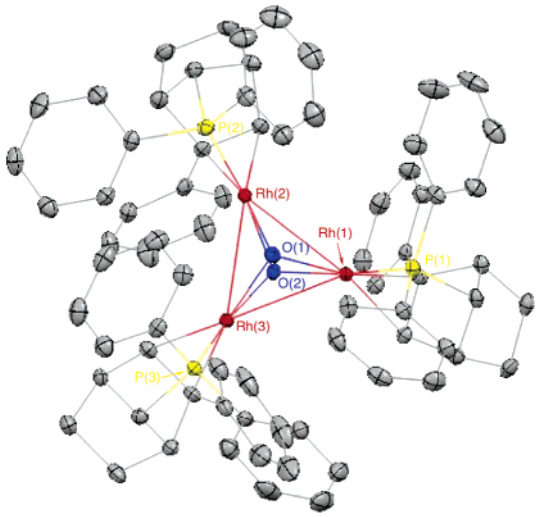

Figure 3. X-ray structure of [Rh_3(μ-O)(μ-OH)((7*S*)-**1a**)$_3$] (**6**) with thermal ellipsoids drawn at the 50% probability level (hydrogens and solvent molecules (CH_2Cl_2) are omitted for clarity). Selected bond lengths (Å) and angles (deg): Rh(1)−P(1) = 2.1515(5), Rh(1)−O(1) = 2.032(1), Rh(1)−O(2) = 2.140(1), Rh(2)−P(2) = 2.1549(5), Rh(2)−O(1) = 2.039(1), Rh(2)−O(2) = 2.138(1), Rh(3)−P(3) = 2.1541(5), Rh(3)−O(1) = 2.047(1), Rh(3)−O(2) = 2.155(1); ∠O(1)−Rh(1)−O(2) = 73.98(5), ∠O(1)−Rh(2)−O(2) = 73.88(5), ∠O(1)−Rh(3)−O(2) = 73.37(5).

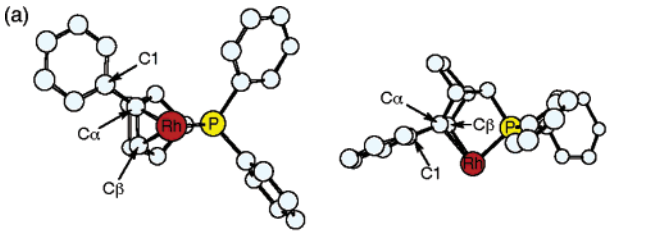

Rh–C1 = 3.01 Å, Rh–Cα = 2.13 Å, Rh–Cβ = 2.09 Å, C1–Cα = 1.48 Å, Cα–Cβ = 1.43 Å; ∠Rh–Cα–C1 = 112°, ∠C1–Cα–Cβ = 126°

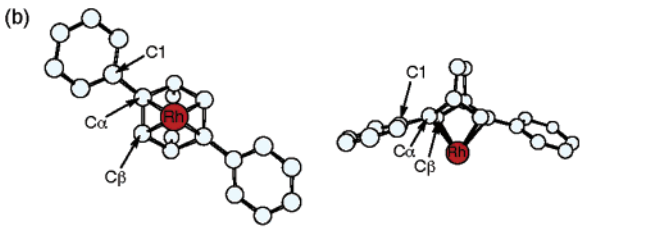

Rh–C1 = 3.05 Å, Rh–Cα = 2.13 Å, Rh–Cβ = 2.10 Å, C1–Cα = 1.50 Å, Cα–Cβ = 1.41 Å; ∠Rh–Cα–C1 = 114°, ∠C1–Cα–Cβ = 125°

Figure 4. Selected bond distances and angles for (a) [Rh_3(μ-O)(μ-OH)((7*S*)-**1a**)$_3$] (**6**) and (b) [RhCl((*R*,*R*)-Ph-bod*)]$_2$.

74°. The ^{31}P NMR of this complex shows a single set of doublet at 73.4 ppm (J_{PRh} = 211 Hz) in dioxane, which may indicate that it stays as a symmetrical trimer in solution as well.

A monomeric representation of complex **6** is shown in Figure 4a to analyze the mode of coordination more in detail. Two phenyl groups on the phosphorus atom equally shield the top-right and bottom-right sections of the space around the rhodium, thereby creating no effective chiral environment around the phosphorus center. In contrast, the steric difference between the phenyl group and the hydrogen atom on the olefin effectively blocks only the top-left section of the space around the rhodium, which may lead to an efficient induction of chirality in asymmetric catalysis. In comparison, the structure of a rhodium complex bearing C_2-symmetric chiral diene (*R*,*R*)-Ph-bod* is illustrated in Figure 4b,[5b] and it is worth noting that the local structure around the olefin of complex **6** is almost identical to that of Rh/(*R*,*R*)-Ph-bod*. Because a Rh/(*R*,*R*)-Ph-bod* complex is known to act as a highly effective catalyst for several carbon−carbon bond forming asymmetric reactions,[5a,5b,5f] the structural similarity in Figure 4 suggests that the Rh/**1a** complex might also display similar efficiency if the stereochemical outcome is dominantly controlled by the olefin portion of the ligand.

Table 1. Rh/(7*S*)-**1**-Catalyzed Asymmetric 1,4-Addition of Arylboronic Acids to α,β-Unsaturated Carbonyl Compounds

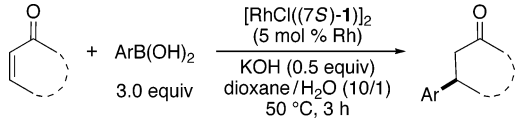

entry	substrate	Ar	ligand	yield (%)	ee (%)[a]	config.
1		Ph	**1a**	91	98 (99)	(*R*)
2		4-MeOC$_6$H$_4$	**1a**	94	98 (98)	(*R*)
3		4-CF$_3$C$_6$H$_4$	**1a**	92	95 (96)	(*R*)
4		2-MeC$_6$H$_4$	**1a**	99	98 (96)	(*R*)
5		Ph	**1a**	94	93 (96)	(*R*)
6	Me, *n*-Pent	Ph	**1a**	91	72 (83)	(*S*)
7[b]		Ph	**1a**	89	97 (95)	(*R*)
8		Ph	**1a**	98	93 (91)	(*R*)
9		Ph	**1b**	90	94	(*R*)
10	NBn	Ph	**1c**	97	95	(*R*)
11		Ph	**1d**	96	93	(*R*)
12		Ph	**1e**	99	84	(*R*)
13		Ph	**1f**	96	91	(*R*)

[a] Numbers in parentheses are the ee values with (*R*,*R*)-Ph-bod* as the ligand (ref 5b). [b] The reaction was conducted for 12 h with 5.0 equiv of $PhB(OH)_2$.

Asymmetric 1,4-Addition Reactions Catalyzed by Rh/(7*S*)-1a. Table 1 summarizes the results of asymmetric 1,4-addition of arylboronic acids to several α,β-unsaturated carbonyl compounds in the presence of a Rh/(7*S*)-**1a** catalyst.[12] In all of the substrate/nucleophile combinations we examined, the 1,4-adducts were obtained in uniformly high chemical yield (89−99% yield). For 2-cyclopenten-1-one, various aromatic groups were effectively installed, giving 3-arylcyclopentanones in high enantiomeric excess (95−98% ee; entries 1−4). Although other cyclic enones such as 2-cyclohexen-1-one also gave the 1,4-adducts with similarly high ee (93% ee; entry 5), acyclic α,β-enones were less effective in this catalyst system, giving the products in somewhat lower enantioselectivity (72% ee; entry 6). This trend of enantioselectivity and the sense of absolute stereoinduction with ligand (7*S*)-**1a** resemble those with (*R*,*R*)-Ph-bod*[5b] (values in parentheses in Table 1), indicating that Rh/(7*S*)-**1a** and Rh/(*R*,*R*)-Ph-bod* display a similar chiral environment during these reactions. In addition to the simple

(12) (a) Takaya, Y.; Ogasawara, M.; Hayashi, T.; Sakai, M.; Miyaura, N. *J. Am. Chem. Soc.* **1998**, *120*, 5579. (b) Hayashi, T.; Takahashi, M.; Takaya, Y.; Ogasawara, M. *J. Am. Chem. Soc.* **2002**, *124*, 5052. For reviews, see: (c) Hayashi, T.; Yamasaki, K. *Chem. Rev.* **2003**, *103*, 2829. (d) Fagnou, K.; Lautens, M. *Chem. Rev.* **2003**, *103*, 169.

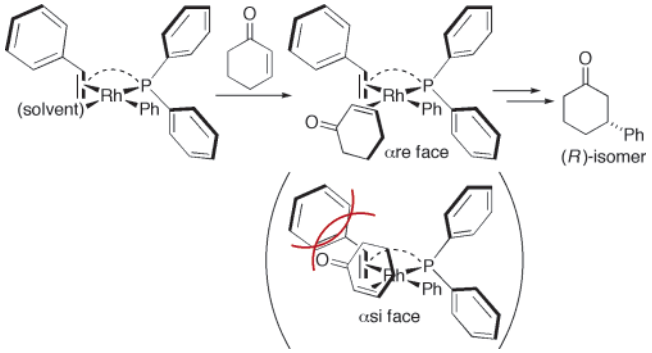

Figure 5. Proposed stereochemical pathway for the Rh/(7*S*)-**1a**-catalyzed asymmetric 1,4-addition of phenylboronic acid to 2-cyclohexen-1-one.

Table 2. Rhodium-Catalyzed Asymmetric 1,4-Addition of Phenylboronic Acid to Maleimide **7**: Ligand Effect on the Regioselectivity

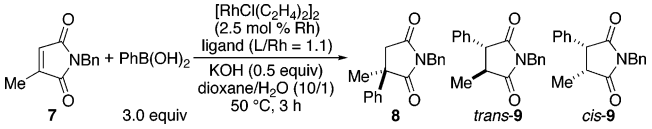

entry	ligand	yield (%)	**8**/**9** (trans/cis)	ee of **8** (%)	ee of **9** (%) (*trans, cis*)
1[a]	(*R*)-binap	99	75/25 (2.1/1)	95	0, 96
2[a]	(*R*,*R*)-Ph-bod*	94	11/89 (1/1.4)	93	79, 99
3[b]	(7*S*)-**1a**	99	17/83 (1/1.2)	77	95, >99

[a] Reported in ref 5g. [b] The reaction was conducted with 5 mol % of catalyst.

α,β-enone substrates, an α,β-unsaturated lactone and a maleimide were also effectively phenylated with high enantiomeric excess (93−97% ee; entries 7 and 8). The degree of enantioselectivity is again in good correlation with (*R*,*R*)-Ph-bod*, showing that the stereochemistry is mainly controlled by the olefin portion of ligand **1a**. In the reaction with 1-benzylmaleimide, the use of phosphine−olefins **1b**−**d**, which have a different diarylphosphino group, did not change the enantioselectivity very much (93−95% ee; entries 9−11), but the change of the olefin substituent (**1e** and **1f**) showed a significant impact on the enantioselectivity (84% ee and 91% ee, respectively; entries 12 and 13). These data are also consistent with the dominant stereocontrol by the olefin chirality of Rh/(7*S*)-**1a**.

On the basis of the results of these 1,4-additions and by analogy with the stereochemical control of a Rh/(*R*,*R*)-Ph-bod* catalyst,[5b] the stereochemical pathway with Rh/(7*S*)-**1a** can be rationalized as shown in Figure 5. Thus, the phenylrhodium species has trans-relationship between the phenyl group and the olefin ligand and the substrate such as 2-cyclohexen-1-one binds to rhodium with its αre face at the cis-position of the olefin ligand, leading to the 1,4-adduct with (*R*)-configuration.

The regioselectivity observed in the rhodium-catalyzed asymmetric 1,4-addition of phenylboronic acid to 1-benzyl-3-methylmaleimide (**7**) highlights the origin of stereochemical control of Rh/(7*S*)-**1a** as well. Thus, as we previously reported,[5g] phenylation of maleimide **7** preferentially gave compound **8** in the presence of chiral bisphosphine ligand (*R*)-binap (Table 2, entry 1), but the use of diene ligand (*R*,*R*)-Ph-bod* produced compounds **9** as the major products (entry 2). The observed regioselectivity was rationalized by the steric interaction between substrate **7** and the ligand substituent that is cis to **7**. When we employed phosphine−olefin (7*S*)-**1a** in this reaction, it gave a similar result as in the reaction with (*R*,*R*)-Ph-bod* (entry 3 vs entry 2). This also suggests that substrate **7** approaches the phenylrhodium species from cis-orientation of the olefin portion of ligand **1a**.

^{31}P NMR Studies on the Catalytic Cycle of the 1,4-Addition Reaction Catalyzed by Rh/(7*S*)-1a. ^{31}P NMR studies on the Rh/(7*S*)-**1a** complexes coordinated with a phenyl group provided significant insight into the structure and reactivity of a phenylrhodium species involved in the catalytic cycle of the 1,4-addition reactions. Thus, a reaction of Rh/(7*S*)-**1a** complex **6** with phenylboronic acid in the presence of PPh_3 as an additional neutral ligand cleanly generated [RhPh(PPh_3)((7*S*)-**1a**)] as a 7:1 mixture of two isomers (**10a** and **10a′**; eq 2). By analyzing the coupling constants of its ^{31}P NMR spectrum (major isomer: $\delta = 50.7$ ppm (dd, $J_{PP} = 339$ Hz and $J_{PRh} = 178$ Hz) and $\delta = 31.7$ ppm (dd, $J_{PP} = 339$ Hz and $J_{PRh} = 154$ Hz); minor isomer: $\delta = 47.9$ ppm (dd, $J_{PRh} = 103$ Hz and $J_{PP} = 27.1$ Hz) and $\delta = 28.4$ ppm (dd, $J_{PRh} = 181$ Hz and $J_{PP} = 27.1$ Hz), see also Figure 6a), we have determined that the major diastereomer with a larger J_{PP} value is complex **10a** with PPh_3 trans to the diphenylphosphino group. Similarly, the use of $P(OMe)_3$ instead of PPh_3 generated [RhPh($P(OMe)_3$)((7*S*)-**1a**)] in the ratio of >15:1 (^{31}P NMR major isomer: $\delta = 138.7$ ppm (dd, $J_{PP} = 507$ Hz and $J_{PRh} = 261$ Hz) and $\delta = 44.3$ ppm (dd, $J_{PP} = 507$ Hz and $J_{PRh} = 154$ Hz); minor isomer: $\delta = 134.8$ ppm (dd, $J_{PRh} = 307$ Hz and $J_{PP} = 44.4$ Hz) and $\delta = 50.9$ ppm (dd, $J_{PRh} = 163$ Hz and $J_{PP} = 44.4$ Hz)), favoring a trans-orientation of $P(OMe)_3$ to the phosphine group (**11a**; eq 3). Considering that an enone could also act as a neutral ligand to rhodium, these results also support the feasibility of the proposed stereochemical orientation in Figure 5.

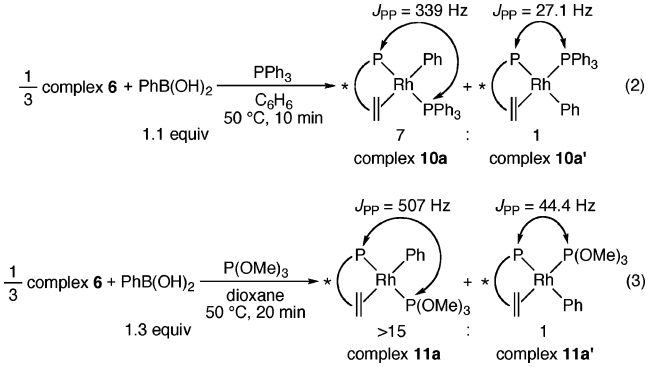

Successful preparation of phenylrhodium complexes **10a**/**10a′** led us to examine several stoichiometric reactions to observe reaction intermediates by using ^{31}P NMR as we previously described for the Rh/binap catalyst system.[12b] Thus, treatment of complexes **10a**/**10a′** (7:1 mixture) with *tert*-butyl vinyl ketone in dioxane at 50 °C for 1 h completely consumed these complexes, and new sets of doublets appeared around 70 ppm along with free PPh_3 at −4.8 ppm (Scheme 2 and Figure 6). These doublet peaks presumably correspond to oxa-π-allylrhodium complexes **12**, based on the result with the Rh/binap system.[12b] Addition of water to this mixture led to replacement of these doublets by a new set of doublet at 73.4 ppm, which is identical to the ^{31}P NMR spectrum of trimer **6** in dioxane. The fact that the PPh_3 peak stayed at −4.8 ppm as a singlet without coordinating to the rhodium suggests that the hydroxorhodium species mostly exists as a trimer in solution. Finally,

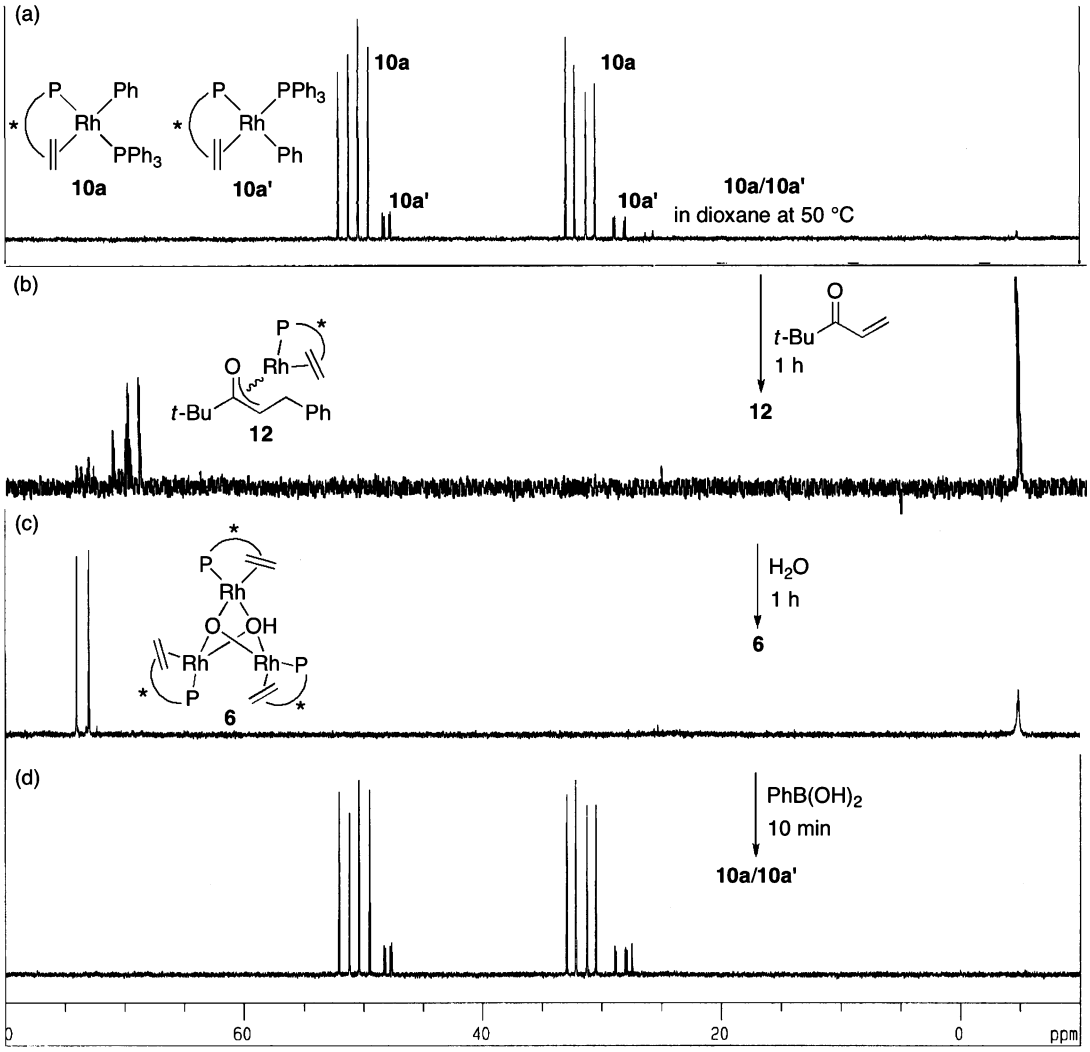

Figure 6. ^{31}P NMR spectra of rhodium complexes in the reactions starting from phenylrhodium **10a**/**10a′**. (a) Phenylrhodium complexes **10a**/**10a′** in 7:1 ratio. (b) Addition of *tert*-butyl vinyl ketone to give oxa-π-allylrhodium complexes **12**. (c) Addition of water to give hydroxorhodium trimer **6**. (d) Addition of phenylboronic acid to give phenylrhodium complexes **10a**/**10a′**.

Scheme 2

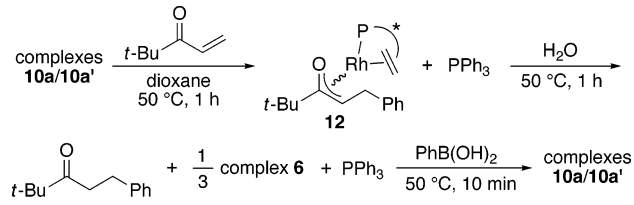

treating this mixture with phenylboronic acid regenerated phenylrhodium species **10a**/**10a′** in the ratio of 7:1.

Kinetic Studies on the 1,4-Addition Reaction Catalyzed by Rh/(7*S*)-1a. A series of experiments were carried out for the kinetic studies of the 1,4-addition of $PhB(OH)_2$ (**13**)[13] to methyl vinyl ketone (MVK (**14**)) in aqueous dioxane in the presence of catalyst complex **6** at 30 °C (eq 4) using a reaction calorimeter (Omnical SuperCRC). The kinetic data were analyzed by the method of reaction progress kinetic analysis developed by Blackmond.[14,15]

We previously observed by the reaction calorimeter that the catalyst activity in this 1,4-addition reaction is highly dependent on the nature of the ligand employed. Thus, the reaction proceeded about 20 times faster with $[Rh(OH)(cod)]_2$ as a catalyst than with $[Rh(OH)(binap)]_2$ at 50 °C,[16] establishing that a diene/rhodium complex has higher catalyst activity than a binap/rhodium complex. Due to its high activity, the reaction catalyzed by $[Rh(OH)(cod)]_2$ can also be conducted at 30 °C, taking about 8.5 min to reach 50% conversion in the presence of 2.7 mM rhodium catalyst (Figure 7).[17]

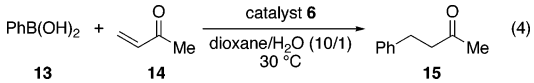

Because ligand **1a** is a hybrid of bisphosphine and diene ligands, it is of interest to examine the catalyst activity of a

(13) In these experiments, phenylboroxine ($(PhBO)_3$) was used as a precursor for phenylboronic acid (**13**). See: Tokunaga, Y.; Ueno, H.; Shimomura, Y.; Seo, T. *Heterocycles* **2002**, *57*, 787 and ref 16.

(14) For excellent reviews, see: (a) Blackmond, D. G. *Angew. Chem., Int. Ed.* **2005**, *44*, 4302. (b) Mathew, J. S.; Klussmann, M.; Iwamura, H.; Valera, F.; Futran, A.; Emanuelsson, E. A. C.; Blackmond, D. G. *J. Org. Chem.* **2006**, *71*, 4711.

(15) (a) Rosner, T.; LeBars, J.; Pfaltz, A.; Blackmond, D. G. *J. Am. Chem. Soc.* **2001**, *123*, 1848. (b) Singh, U. K.; Strieter, E. R.; Blackmond, D. G.; Buchwald, S. L. *J. Am. Chem. Soc.* **2002**, *124*, 14104. (c) Mathew, S. P.; Gunathilagan, S.; Roberts, S. M.; Blackmond, D. G. *Org. Lett.* **2005**, *7*, 4847.

(16) (a) Kina, A.; Iwamura, H.; Hayashi, T. *J. Am. Chem. Soc.* **2006**, *128*, 3904. (b) Kina, A.; Yasuhara, Y.; Nishimura, T.; Iwamura, H.; Hayashi, T. *Chem. Asian J.* **2006**, *1*, 707.

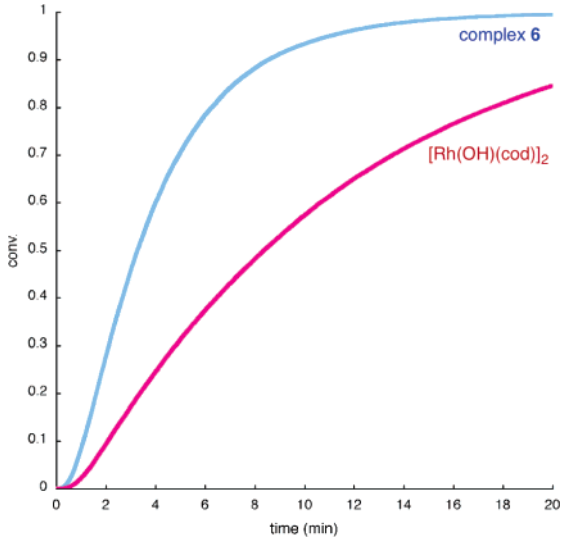

Figure 7. Conversion vs time for the reactions of **13** ($[\mathbf{13}]_0 = 67$ mM) with **14** ($[\mathbf{14}]_0 = 201$ mM) in 1,4-dioxane/H_2O (3.0 mL/0.3 mL) in the presence of a rhodium catalyst ($[Rh]_{total} = 2.7$ mM) at 30 °C. Red: [Rh(OH)(cod)]$_2$ as the catalyst in the presence of $[B(OH)_3]_0 = 536$ mM; blue: complex **6** as the catalyst.

Rh/**1a** complex. Interestingly, the reaction catalyzed by Rh/(7*S*)-**1a** complex **6** exhibited somewhat faster reaction rate than the Rh/cod-catalyzed reaction under similar conditions at 30 °C, taking only 3 min for 50% conversion.[18] This result shows that the catalyst activity of Rh/**1a** is closer to Rh/cod rather than to Rh/binap, indicating that the olefin portion of ligand **1a** is mainly responsible for determining its catalyst activity.

Figure 8 summarizes the results of a series of experiments for obtaining kinetic parameters in the 1,4-addition reaction catalyzed by complex **6**, where the *x*-axis is the concentration of PhB(OH)$_2$ (**13**) and the *y*-axis is the reaction rate (the reactions progress from right to left). The curves for two experiments carried out at the same "excess"[19] (a and b) are well overlaid with each other, indicating that the reaction system has no catalyst deactivation or product inhibition. The results of different "excess"[19] experiments (a, c, and d) establish that the reaction rate shows first-order dependence on [PhB(OH)$_2$ (**13**)] and pseudo zero-order on [MVK (**14**)], and these values are the same as those in the reaction catalyzed by Rh/binap[16a] or by Rh/cod.[16b]

However, unlike the order in the Rh/binap catalyst (≈0.5) or the Rh/cod catalyst (0.65), the order in the Rh/**1a** catalyst was determined to be 0.4, which is demonstrated by the overlapping plots of rate/$[Rh]_{total}^{0.4}$ versus [PhB(OH)$_2$ (**13**)] (inset in Figure 8). In the case of Rh/binap, the catalyst order (close to 0.5) was explained by the existence of an inactive dimer−active monomer equilibrium with a large equilibrium constant K_{dimer}, and in the case of Rh/cod, the order 0.65 was similarly explained with significant contribution of the monomeric species in solution. But in the present catalyst system, the value 0.4 (significantly smaller than 0.5) cannot be explained by the involvement of a dimer−monomer equilibrium. The fact that complex **6** is a trimeric species in a solid state (Figure 3) and that 0.4 is close to 0.33 strongly suggests that the catalyst has an inactive trimer−active monomer equilibrium under the reaction conditions and the rhodium species dominantly stays as a trimer during the catalytic process. Thus, the catalytic cycle of the present reaction system can be illustrated as shown in Scheme 3 and the equilibrium constant between trimer **6** and monomer **16** (K_{trimer}) should be large. On the basis of the reaction orders of [PhB(OH)$_2$ (**13**)] and [MVK (**14**)] (first and zero, respectively), the turnover-limiting step is the formation of the phenylrhodium species (**17**) and the subsequent insertion step is much faster. Under these conditions where k_2[MVK (**14**)] ≫ k_1[PhB(OH)$_2$ (**13**)] applies, the rate equation can be expressed as shown in eq 5.

$$v = k_1[\mathbf{13}][\mathbf{16}] = \frac{k_1[\mathbf{13}][Rh]_{total}^{1/3}}{(3K_{trimer})^{1/3}} \quad (5)$$

Nonlinear Effect Studies on the Asymmetric 1,4-Addition Catalyzed by Rh/1a. The fact that majority of the Rh/(7*S*)-**1a** species stays in a trimeric form during the catalysis suggests the possibility of nonlinear effect (NLE) under the present reaction conditions, which has never been studied in detail with a catalyst having a monomer−trimer equilibrium.[20] As a starting point, we confirmed by ^{31}P NMR that only the homochiral trimers (*SSS*-**6** and *RRR*-**6**) are generated even when non-enantiopure ligand **1a** is used in the reaction with [Rh(OH)(cod)]$_2$, indicating that a negative NLE in ee_{prod} and an amplified reaction rate are expected with a β-substituted substrate such as 2-cyclohexen-1-one. By conducting 1,4-additions to 2-cyclohexen-1-one with catalysts of various ee, a negative NLE and an amplified reaction rate were actually observed as depicted in Figure 9. Considering that the formation of the heterochiral trimers (*SSR*-**6** and *SRR*-**6**) is negligible (Scheme 4), concentrations of monomers [*S*-**16**] and [*R*-**16**] are readily calculated using the K_{trimer} value for the homochiral trimers.[21] The equations for ee_{prod} and the reaction rate (v_{ee}) are defined by the concentrations of active monomeric rhodium complexes [*S*-**16**] and [*R*-**16**] as shown in eq 6,

$$ee_{prod} = ee_{100\%ee}\frac{[S\text{-}\mathbf{16}] - [R\text{-}\mathbf{16}]}{[S\text{-}\mathbf{16}] + [R\text{-}\mathbf{16}]}$$

$$\frac{v_{ee}}{v_{100\%ee}} = \frac{[S\text{-}\mathbf{16}] + [R\text{-}\mathbf{16}]}{[S\text{-}\mathbf{16}]_{100\%ee}} \quad (6)$$

where $ee_{100\%ee}$ (93% ee) and $v_{100\%ee}$ are the enantioselectivity and the rate of the reaction with an enantiopure catalyst, respectively.[20c,22] By fitting eq 6 to the experimental results in Figure 9, the trimerization constant was estimated to be $K_{trimer} = 9 \times 10^5$ M^{-2}. Using this K_{trimer} value, eq 5 (black solid lines) shows good fits when $k_1 = 5$ M^{-1}s^{-1} with experimental results in Figure 8 during 50−80% conversions after the induction

(17) The reaction was carried out in the presence of an excess amount of B(OH)$_3$. In the absence of B(OH)$_3$, the reaction proceeds in a slower rate.
(18) The reaction was carried out in the absence of B(OH)$_3$. In the presence of B(OH)$_3$, the maximum reaction rate is still larger than that with Rh/cod, but it shows a significant induction period.
(19) Following the method developed by Blackmond, the "excess" here refers to the difference of the concentration of methyl vinyl ketone [**14**] and the concentration of phenylboronic acid [**13**] ("excess" = [**14**] − [**13**] = $[\mathbf{14}]_0$ − $[\mathbf{13}]_0$). For a detailed utility of this concept, see ref 14.
(20) (a) Puchot, C.; Samuel, O.; Dunach, E.; Zhao, S.; Agami, C.; Kagan, H. B. *J. Am. Chem. Soc.* **1986**, *108*, 2353. For reviews, see: (b) Girard, C.; Kagan, H. B. *Angew. Chem., Int. Ed.* **1998**, *37*, 2922. (c) Blackmond, D. G. *Acc. Chem. Res.* **2000**, *33*, 402.
(21) See Supporting Information for details.
(22) (a) Kitamura, M.; Okada, S.; Suga, S.; Noyori, R. *J. Am. Chem. Soc.* **1989**, *111*, 4028. (b) Kitamura, M.; Suga, S.; Oka, H.; Noyori, R. *J. Am. Chem. Soc.* **1998**, *120*, 9800.

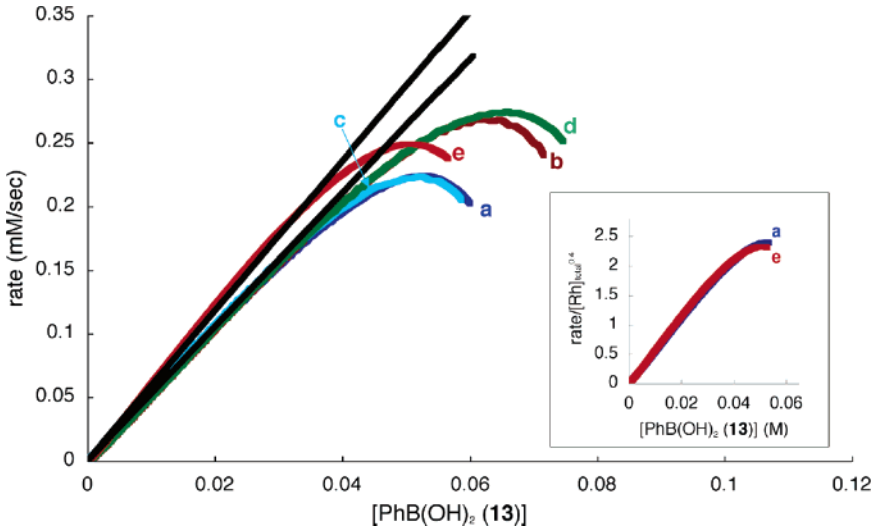

Figure 8. Rate vs [**13**] and rate/$[Rh]_{total}^{0.4}$ vs [**13**] (inset) for the reactions of **13** with **14** in 1,4-dioxane (3.0 mL) and H_2O (0.3 mL) in the presence of catalyst **6** at 30 °C. The progress of the reaction runs from right to left in these figures. The solid lines represent the calculated rate vs [**13**] given in eq 5. Reaction conditions: (a) $[\mathbf{13}]_0 = 67$ mM, $[\mathbf{14}]_0 = 201$ mM, $[\mathbf{6}]_0 = 2.7$ mM Rh; (b) $[\mathbf{13}]_0 = 80$ mM, $[\mathbf{14}]_0 = 214$ mM, $[\mathbf{6}]_0 = 2.7$ mM Rh; (c) $[\mathbf{13}]_0 = 67$ mM, $[\mathbf{14}]_0 = 101$ mM, $[\mathbf{6}]_0 = 2.7$ mM Rh; (d) $[\mathbf{13}]_0 = 85$ mM, $[\mathbf{14}]_0 = 201$ mM, $[\mathbf{6}]_0 = 2.7$ mM Rh; (e) $[\mathbf{13}]_0 = 67$ mM, $[\mathbf{14}]_0 = 201$ mM, $[\mathbf{6}]_0 = 3.8$ mM Rh.

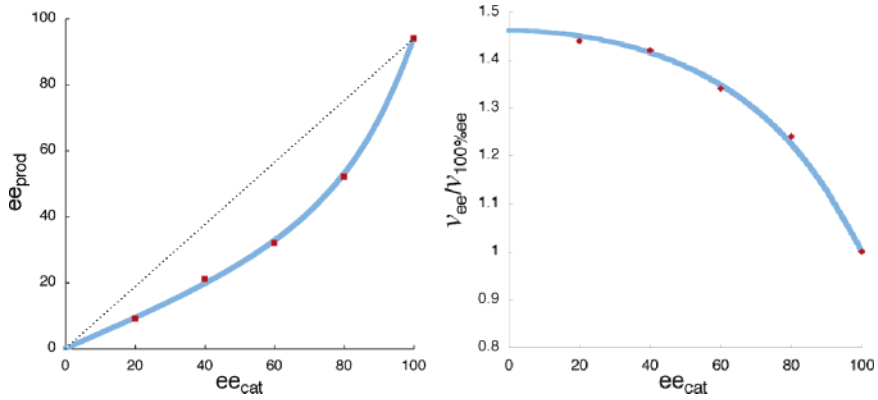

Figure 9. ee_{prod} vs ee_{cat} (left) and $v_{ee}/v_{100\%ee}$ vs ee_{cat} (right): observation (red squares) and simulation (blue solid line) of the nonlinear effect in the reaction of **13** with 2-cyclohexen-1-one catalyzed by Rh/**1a**.

Scheme 3. Proposed Catalytic Cycle for the Rh/**1a**-Catalyzed 1,4-Addition of Phenylboronic Acid (**13**) to Methyl Vinyl Ketone (**14**) ([Rh] = Rh/**1a**)

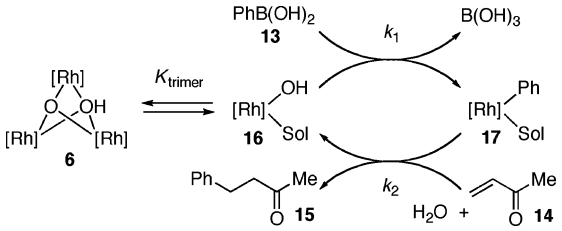

Scheme 4

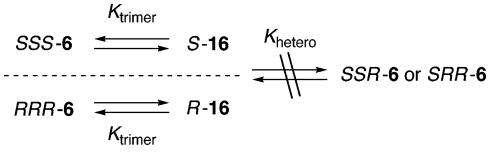

period.[23] It is worth noting that the rate constant for the transmetalation k_1 in this system is significantly larger than the corresponding rate constant with a Rh/cod catalyst ($k_1 = 1.3$ $M^{-1}s^{-1}$), and this conclusion is consistent with the time-dependent conversion graph of $PhB(OH)_2$ (**13**) to 4-phenyl-2-butanone (**15**) in Figure 7.

Conclusions

We have described a full overview on the use of chiral phosphine−olefin ligands **1** in the rhodium-catalyzed asymmetric 1,4-addition of arylboronic acids to α,β-unsaturated carbonyl compounds. Through the kinetic studies using a reaction calorimeter, we have determined that the Rh/**1** catalyst has very high catalytic activity in these reactions, and that its activity is higher than a Rh/cod catalyst, which is considered to be one of the most active catalysts in the rhodium-catalyzed 1,4-addition reactions. It has also been demonstrated that the enantioselectivity of Rh/**1a** is as high as Rh/Ph-bod*, and that transmetalation occurs at the trans-position to the olefin ligand of Rh/**1** and the stereochemical outcome is controlled at the cis-position to the olefin. By the use of ^{31}P NMR spectroscopy, it has been shown that the catalytic cycle with Rh/**1** is essentially the same as the one with Rh/binap, but it involves a trimer−monomer equilibrium of the catalyst, rather than a dimer−monomer equilibrium, which has been confirmed by the kinetic studies with a reaction calorimeter. We have also succeeded

(23) Kinetic modeling of the data to fit the proposed rate expression in eq 5 was carried out using the Excel least-squares program.

for the first time in observing a negative nonlinear effect derived from an inactive trimer−active monomer equilibrium of the catalyst.

Experimental Section

General. All air- and moisture-sensitive manipulations were carried out with standard Schlenk techniques under nitrogen or in a glove box under argon. Benzene, hexane, and 1,4-dioxane were distilled over benzophenone ketyl under nitrogen. Dichloromethane was distilled over CaH_2 under nitrogen. Phosphine−olefins **1a** and **1f** were synthesized following the literature procedures.[8] Phosphine−olefins **1b**−**1e** were synthesized in a similar manner following the procedure for **1a**.[8] [Rh(OH)(cod)]$_2$[24] and [RhCl((7*S*)-**1a**)]$_2$[8] were synthesized following the literature procedures.

Analytical Data for Phosphine−Olefins 1. (1*S*,4*R*,7*S*)-(−)-7-Diphenylphosphino-2-phenylbicyclo[2.2.1]hept-2-ene (1a): ^{1}H NMR ($CDCl_3$): δ 7.45−7.35 (m, 5H), 7.35−7.22 (m, 9H), 7.19 (t,$^3J_{HH}$ = 7.3 Hz, 1H), 6.31 (d,$^3J_{HH}$ = 2.8 Hz, 1H), 3.18 (s, 1H), 2.97 (s, 1H), 2.49 (d,$^3J_{HH}$ = 6.8 Hz, 1H), 1.95−1.80 (m, 2H), 1.33−1.20 (m, 2H). ^{13}C NMR ($CDCl_3$): δ 146.4 (d,$^3J_{CP}$ = 4.1 Hz), 139.7 (d,$^1J_{CP}$ = 48.7 Hz), 139.6 (d,$^1J_{CP}$ = 48.5 Hz), 135.4, 133.0 (d,$^2J_{CP}$ = 19.1 Hz), 132.9 (d,$^2J_{CP}$ = 19.2 Hz), 128.40, 128.35, 128.29 (d,$^3J_{CP}$ = 2.5 Hz), 128.28 (d,$^3J_{CP}$ = 3.1 Hz), 128.2, 128.1 ($^3J_{CP}$ = 3.6 Hz), 127.0, 125.3, 61.8 (d,$^1J_{CP}$ = 5.1 Hz), 47.2 (d,$^2J_{CP}$ = 6.6 Hz), 47.1 (d,$^2J_{CP}$ = 6.6 Hz), 27.8 (d,$^3J_{CP}$ = 3.6 Hz), 25.9 (d,$^3J_{CP}$ = 4.1 Hz). ^{31}P{^{1}H} NMR ($CDCl_3$): δ −17.1 (s). $[\alpha]^{20}_D$ −287 (*c* 0.40, CH_2Cl_2). Anal. Calcd for $C_{25}H_{23}P$: C, 84.72; H, 6.54. Found: C, 84.77; H, 6.79.

(1*S*,4*R*,7*S*)-(−)-7-Di(4-methoxyphenyl)phosphino-2-phenylbicyclo-[2.2.1]hept-2-ene (1b): ^{1}H NMR ($CDCl_3$): δ 7.39 (d,$^3J_{HH}$ = 7.4 Hz, 2H), 7.34 (dd,$^3J_{HH}$ = 8.5 Hz and$^3J_{PH}$ = 7.0 Hz, 2H), 7.29 (t,$^3J_{HH}$ = 7.5 Hz, 2H), 7.25 (dd,$^3J_{HH}$ = 8.6 Hz and$^3J_{PH}$ = 7.4 Hz, 2H), 7.20 (t,$^3J_{HH}$ = 7.3 Hz, 1H), 6.88 (d,$^3J_{HH}$ = 8.7 Hz, 2H), 6.83 (d,$^3J_{HH}$ = 8.8 Hz, 2H), 6.30 (d,$^3J_{HH}$ = 3.0 Hz, 1H), 3.80 (s, 3H), 3.78 (s, 3H), 3.16 (s, 1H), 2.94 (s, 1H), 2.43 (d,$^2J_{PH}$ = 6.9 Hz, 1H), 1.93−1.81 (m, 2H), 1.31−1.24 (m, 2H). ^{13}C NMR ($CDCl_3$): δ 159.8, 146.3 (d,$^3J_{CP}$ = 3.5 Hz), 135.3, 134.2 (d,$^2J_{CP}$ = 21.2 Hz), 134.1(d,$^2J_{CP}$ = 20.2 Hz), 130.6 (d,$^1J_{CP}$ = 61.6 Hz), 130.5 (d,$^1J_{CP}$ = 60.4 Hz), 128.3, 128.1 (d,$^3J_{CP}$ = 3.6 Hz), 126.9, 125.2, 114.0 (d,$^3J_{CP}$ = 7.3 Hz), 113.9 (d,$^3J_{CP}$ = 7.8 Hz), 62.1 (d,$^1J_{CP}$ = 4.8 Hz), 55.09, 55.08, 47.0 (d,$^2J_{CP}$ = 10.9 Hz), 46.9 (d,$^2J_{CP}$ = 10.9 Hz), 27.9 (d,$^3J_{CP}$ = 3.1 Hz), 25.9 (d,$^3J_{CP}$ = 4.1 Hz). ^{31}P{^{1}H} NMR ($CDCl_3$): δ −20.9 (s). $[\alpha]^{20}_D$ −263 (*c* 0.40, CH_2Cl_2). Anal. Calcd for $C_{27}H_{27}O_2P$: C, 78.24; H, 6.57. Found: C, 78.05; H, 6.66.

(1*S*,4*R*,7*S*)-(−)-7-Di(4-trifluoromethylphenyl)phosphino-2-phenylbicyclo[2.2.1]hept-2-ene (1c): ^{1}H NMR ($CDCl_3$): δ 7.59 (d,$^3J_{HH}$ = 7.8 Hz, 2H), 7.53 (d,$^3J_{HH}$ = 7.8 Hz, 2H), 7.49 (t,^3J = 7.1 Hz, 2H), 7.40 (t,^3J = 7.0 Hz, 2H), 7.37 (d,$^3J_{HH}$ = 8.4 Hz, 2H), 7.31 (t,$^3J_{HH}$ = 7.4 Hz, 2H), 7.23 (t,$^3J_{HH}$ = 7.1 Hz, 1H), 6.32 (d,$^3J_{HH}$ = 2.4 Hz, 1H), 3.19 (s, 1H), 2.99 (s, 1H), 2.49 (d,$^2J_{PH}$ = 6.6 Hz, 1H), 1.99−1.87 (m, 2H), 1.40−1.28 (m, 2H). ^{13}C NMR ($CDCl_3$): δ 146.7, 144.2 (d,$^1J_{CP}$ = 23.8 Hz), 144.0 (d,$^1J_{CP}$ = 21.2 Hz), 134.9, 133.2 (d,$^2J_{CP}$ = 20.7 Hz), 133.0 (d,$^2J_{CP}$ = 20.2 Hz), 130.6 (q,$^2J_{CF}$ = 32.1 Hz), 128.5, 127.8 (d,$^3J_{CP}$ = 3.6 Hz), 127.3, 125.1, 124.1 (q,$^1J_{CF}$ = 271.2 Hz), 61.5 (d,$^1J_{CP}$ = 5.1 Hz), 47.3, 47.2, 27.6 (d,$^3J_{CP}$ = 3.6 Hz), 25.7 (d,$^3J_{CP}$ = 3.1 Hz). ^{31}P-{^{1}H} NMR ($CDCl_3$): δ −15.7 (s). $[\alpha]^{20}_D$ −214 (*c* 0.65, CH_2Cl_2). Anal. Calcd for $C_{27}H_{21}F_6P$: C, 66.12; H, 4.32. Found: C, 66.21; H, 4.47.

(1*S*,4*R*,7*S*)-(−)-7-Dibenzophosphoryl-2-phenylbicyclo[2.2.1]hept-2-ene (1d): ^{1}H NMR ($CDCl_3$): δ 7.90 (d,$^3J_{HH}$ = 7.7 Hz, 1H), 7.89 (d,$^3J_{HH}$ = 7.8 Hz, 1H), 7.76 (dd,$^3J_{HH}$ = 7.5 Hz and$^3J_{PH}$ = 4.5 Hz, 1H), 7.63 (dd,$^3J_{HH}$ = 6.8 Hz and$^3J_{PH}$ = 4.6 Hz, 1H), 7.56 (d,$^3J_{HH}$ = 7.7 Hz, 2H), 7.44 (t,$^3J_{HH}$ = 7.3 Hz, 1H), 7.42 (t,$^3J_{HH}$ = 7.2 Hz, 1H), 7.39 (t,$^3J_{HH}$ = 7.7 Hz, 2H), 7.37−7.33 (m, 1H), 7.31−7.29 (m, 1H), 7.28 (t,$^3J_{HH}$ = 7.4 Hz, 1H), 6.47 (d,$^3J_{HH}$ = 3.0 Hz, 1H), 3.49 (s, 1H), 3.23 (s, 1H), 1.71−1.63 (m, 2H), 1.58 (d,$^2J_{PH}$ = 6.2 Hz, 1H), 1.32−1.23 (m, 2H). ^{13}C NMR ($CDCl_3$): δ 146.1 (d,$^3J_{CP}$ = 3.6 Hz) 144.43 (d,$^1J_{CP}$ = 30.0 Hz), 144.38 (d,$^1J_{CP}$ = 29.0 Hz), 143.61 (d,$^2J_{CP}$ = 8.8 Hz), 143.60 (d,$^2J_{CP}$ = 9.4 Hz), 135.4, 130.4 (d,$^2J_{CP}$ = 14.4 Hz), 130.2 (d,$^2J_{CP}$ = 13.9 Hz), 128.6, 128.2 (d,$^3J_{CP}$ = 3.5 Hz), 128.1, 127.2, 126.97 (d,$^3J_{CP}$ = 7.3 Hz), 126.96 (d,$^3J_{CP}$ = 7.8 Hz), 125.2, 121.18, 121.15, 63.1 (d,$^1J_{CP}$ = 10.9 Hz), 47.3 (d,$^2J_{CP}$ = 9.9 Hz), 47.2 (d,$^2J_{CP}$ = 10.4 Hz), 27.4 (d,$^3J_{CP}$ = 4.1 Hz), 25.4 (d,$^3J_{CP}$ = 4.1 Hz). ^{31}P{^{1}H} NMR ($CDCl_3$): δ −16.5 (s). $[\alpha]^{20}_D$ −428 (*c* 0.16, CH_2Cl_2). HRMS (ESI) calcd for $C_{25}H_{22}P$ (M+H$^+$) 353.1454, found 353.1456.

(1*S*,4*R*,7*S*)-(−)-7-Diphenylphosphino-2-(3,5-dimethylphenyl)bicyclo-[2.2.1]hept-2-ene (1e): ^{1}H NMR ($CDCl_3$): δ 7.39 (t,^3J = 7.3 Hz, 2H), 7.33−7.27 (m, 8H), 7.02 (s, 2H), 6.86 (s, 1H), 6.28 (d,$^3J_{HH}$ = 2.8 Hz, 1H), 3.18 (s, 1H), 2.95 (s, 1H), 2.48 (d,$^2J_{PH}$ = 6.9 Hz, 1H), 2.29 (s, 6H), 1.92−1.83 (m, 2H), 1.32−1.24 (m, 2H). ^{13}C NMR ($CDCl_3$): δ 146.6 (d,$^3J_{CP}$ = 3.5 Hz), 139.8 (d,$^1J_{CP}$ = 43.9 Hz), 139.6 (d,$^1J_{CP}$ = 43.4 Hz), 137.8, 135.2, 133.0 (d,$^2J_{CP}$ = 19.7 Hz), 132.9 (d,$^2J_{CP}$ = 19.2 Hz), 128.8, 128.3 (d,$^3J_{CP}$ = 6.1 Hz), 128.23, 128.21 (d,$^3J_{CP}$ = 6.1 Hz), 128.20, 127.8 (d,$^3J_{CP}$ = 4.1 Hz), 123.1, 62.1 (d,$^1J_{CP}$ = 4.8 Hz), 55.09, 55.08, 47.0 (d,$^2J_{CP}$ = 10.9 Hz), 46.9 (d,$^2J_{CP}$ = 10.9 Hz), 27.9 (d,$^3J_{CP}$ = 3.1 Hz), 25.9 (d,$^3J_{CP}$ = 4.1 Hz). ^{31}P{^{1}H} NMR ($CDCl_3$): δ −17.2 (s). $[\alpha]^{20}_D$ −249 (*c* 0.43, CH_2Cl_2). Anal. Calcd for $C_{27}H_{27}P$: C, 84.79; H, 7.12. Found: C, 85.04; H, 6.96.

(1*S*,4*R*,7*S*)-(−)-7-Diphenylphosphino-2-benzylbicyclo[2.2.1]hept-2-ene (1f): ^{1}H NMR ($CDCl_3$): δ 7.38−7.34 (m, 2H), 7.32−7.17 (m, 11H), 7.12−7.09 (m, 2H), 5.59 (s, 1H), 3.44 (d,$^2J_{HH}$ = 15.3 Hz, 1H), 3.40 (d,$^2J_{HH}$ = 15.4 Hz, 1H), 2.79 (s, 1H), 2.52 (s, 1H), 2.28 (d,$^3J_{HH}$ = 7.2 Hz, 1H), 1.82−1.74 (m, 1H), 1.65−1.58 (m, 1H), 1.25−1.16 (m, 1H), 1.05−0.95 (m, 1H). ^{13}C NMR ($CDCl_3$): δ 147.0 (d,$^3J_{CP}$ = 3.1 Hz), 139.9 (d,$^1J_{CP}$ = 43.9 Hz), 139.7 (d,$^1J_{CP}$ = 43.4 Hz), 139.2, 133.0 (d,$^2J_{CP}$ = 19.1 Hz), 132.7 (d,$^2J_{CP}$ = 19.2 Hz), 129.37, 129.36, 128.24 (d,$^3J_{CP}$ = 6.1 Hz), 128.23, 128.13 (d,$^3J_{CP}$ = 4.1 Hz), 128.09, 127.9 ($^3J_{CP}$ = 4.1 Hz), 125.9, 62.2 (d,$^1J_{CP}$ = 5.1 Hz), 48.5 (d,$^2J_{CP}$ = 12.4 Hz), 46.3 (d,$^2J_{CP}$ = 12.9 Hz), 36.9, 27.9 (d,$^3J_{CP}$ = 3.6 Hz), 25.6 (d,$^3J_{CP}$ = 4.1 Hz). ^{31}P{^{1}H} NMR ($CDCl_3$): δ −17.5 (s). $[\alpha]^{20}_D$ −56.5 (*c* 0.56, CH_2Cl_2). Anal. Calcd for $C_{26}H_{25}P$: C, 84.75; H, 6.84. Found: C, 84.96; H, 7.10.

Preparation of [Rh$_3$(μ-O)(μ-OH)((7*S*)-1a)$_3$] (6). A mixture of [Rh(OH)(cod)]$_2$ (68.4 mg, 0.300 mmol Rh) and (*7S*)-**1a** (106 mg, 0.300 mmol) in benzene (15 mL) was stirred for 5 h at 50 °C, and the solvent was removed under vacuum. The residue was dissolved in dichloromethane (8 mL) and filtered through PTFE membrane (0.45 μm). The remaining solution was diluted with hexane (30 mL) to form a precipitate, and it was collected by filtering off the solvent and dried under vacuum to afford an orange solid (100 mg, 0.071 mmol, 71% yield), which was further recrystallized from dichloromethane/hexane to furnish single crystals suitable for X-ray analysis.

^{1}H NMR (C_6D_6): δ 8.45 (dd,$^3J_{HH}$ = 10.5 and 8.3 Hz, 6H), 8.11 (dd,$^3J_{HH}$ = 10.7 and 8.4 Hz, 6H), 7.30−7.10 (m, 15H), 6.85 (t,$^3J_{HH}$ = 7.5 Hz, 3H), 6.79 (t,$^3J_{HH}$ = 7.3 Hz, 6H), 6.63 (t,$^3J_{HH}$ = 6.9 Hz, 3H), 6.55 (t,$^3J_{HH}$ = 7.1 Hz, 6H), 3.33 (s, 3H), 2.94 (s, 3H), 2.76 (s, 3H), 1.82−1.76 (m, 3H), 1.68 (s, 3H), 1.57−1.52 (m, 3H), 1.41−1.28 (m, 6H), −3.10 (s, 1H). ^{31}P{^{1}H} NMR (C_6D_6): δ 73.2 (d,$^1J_{RhP}$ = 211 Hz). Anal. Calcd for $C_{75}H_{67}O_2P_3Rh_3$: C, 64.25; H, 4.82. Found: C, 64.52; H, 5.06.

General Procedure for Rh/(7S)-1a-Catalyzed Asymmetric 1,4-Addition (Tables 1 and 2). KOH (0.10 mL, 0.10 mmol; 1.0 M aqueous) was added to a solution of [RhCl((7*S*)-**1a**)]$_2$ (4.9 mg, 10 mmol Rh) in 1,4-dioxane (0.50 mL), and the resulting solution was stirred for 5 min at room temperature. ArB(OH)$_2$ (0.60 mmol) and an α,β-unsaturated compound (0.20 mmol) were then added to it with additional 1,4-dioxane (0.50 mL), and the resulting mixture was stirred for 3 h at 50 °C. After passing through a pad of silica gel with EtOAc, the solvent was removed under vacuum. The residue was chromatographed on silica gel with EtOAc/hexane to afford the 1,4-adduct.

Acknowledgment. Support has been provided in part by a Grant-in-Aid for Scientific Research, the Ministry of Education,

(24) Uson, R.; Oro, L. A.; Cabeza, J. A. *Inorg. Synth.* **1985**, *23*, 126.

Culture, Sports, Science and Technology, Japan (21 COE on Kyoto University Alliance for Chemistry).

Supporting Information Available: Experimental procedures for kinetic studies using reaction calorimetry and their analyses and X-ray data for complex **6**. These materials are available free of charge via the Internet at http://pubs.acs.org.

JA0671013